electrochem

MDPI

Article

Modelling of Biotrickling Filters for Treatment of NO_x Analytical Expressions for the NO_x Concentration in Both Gas and Biofilm Phases

Ramasamy Umadevi [1], Ponraj Jeyabarathi [2], Kothandapani Venugopal [1], Michael E. G. Lyons [3,*] and Lakshmanan Rajendran [4]

[1] PG & Research Department of Mathematics, Government Arts College, Bharathidasan University, Tiruchirappalli 639120, India; umaraj1966@gmail.com (R.U.); drvenugopal2013@gmail.com (K.V.)
[2] Department of Mathematics, Government Arts College, Bharathidasan University, Tiruchirappalli 621713, India; bsc.jeya@yahoo.com
[3] School of Chemistry and AMBER National Centre, Trinity College Dublin, University of Dublin, D02 PN40 Dublin, Ireland
[4] Department of Mathematics, AMET (Deemed to Be University), Chennai 603112, India; raj_sms@rediffmail.com
* Correspondence: melyons@tcd.ie

Abstract: A mathematical model of an ideal biotrickling filter (BF) system that inoculates a recently identified strain of *Chelatococcus daeguensis* TAD1 and brings about efficient nitrogen oxide treatment is discussed. The proposed model is based on nonlinear mass transport equations at the gas–biofilm interface. Using Akbari–Ganji's technique, approximate analytical expressions for the nitric oxide concentration in the gaseous and biofilm phases were developed for all feasible system parameters. In addition, to investigate the dynamic behaviour of the system, a numerical analysis of the problem is provided using MATLAB tools. To demonstrate this new approach, graphical data are provided and quantitatively discussed. This theoretical result has good agreement with the numerical simulation (MATLAB) results for the experimental values of parameters.

Keywords: mathematical model; numerical simulation; nitrogen oxide; biotrickling; Akbari–Ganji's method (AGM)

Citation: Umadevi, R.; Jeyabarathi, P.; Venugopal, K.; Lyons, M.E.G.; Rajendran, L. Modelling of Biotrickling Filters for Treatment of NO_x Analytical Expressions for the NO_x Concentration in Both Gas and Biofilm Phases. *Electrochem* **2022**, *3*, 361–378. https://doi.org/10.3390/electrochem3030025

Academic Editor: Masato Sone

Received: 19 May 2022
Accepted: 24 June 2022
Published: 5 July 2022

1. Introduction

In biotrickling filters, the biological treatment of contaminated air requires a complex combination of physical, chemical, and biological processes. It can be challenging to predict how biotrickling filters will behave under various conditions. Fortunately, computers and mathematical models are far more capable than the human mind at tracking many complex relationships. Mathematical models of biotrickling filtration can thus be beneficial in research and design. Additionally, these models facilitate the creation of a basic understanding of the process and technical tasks, such as reactor design, scaleup, and process optimization [1].

The modelling process implies some translation of concepts into equations that can be solved. In most cases, the modelling of biotrickling filters involves mass balances of the contaminant(s), oxygen, and products resulting from contaminant degradation. These include the gas phase, a solid phase, and biofilm and liquid phases in the case of biotrickling filters. Depending on the model concept and assumptions, the resulting equations may include terms for the accumulation of reactive products (i.e., odours, VOCs, oxygen, nitrogen oxide, nutrients, and by-products) in all phases, dispersion effects in air, mass transfer between the air and biofilm phases, diffusional mass transfer in the biofilm, consumption due to biological oxidation, adsorption onto solid media, biomass growth, the physiological state of the biomass, etc. [1]. Thus, the resulting model often comprises a

complex set of nonlinear partial differential equations with initial and boundary conditions. Most of the time, exact analytical solutions are difficult or impossible, and methods are used with the appropriate numerical algorithms to obtain solutions to the model instead.

More recently, Kalandar et al. [2] developed a comprehensive dynamic mathematical model consisting of mass transfer through gas, liquid, and biofilm phases with the kinetics of biodegradation in the BTF and accumulation of methanol in the liquid. A mathematical model for the simulation of the removal of hydrophilic compounds using biotrickling filtration was developed by San-Valero [3].

Biotrickling filters can effectively be used in NO removal. Many researchers have used the process to treat nitrogen oxide (NOx)-contaminated gas via denitrification [4,5]. The emission of nitrogen oxides (NOx) and their induced secondary contaminants is harmful to human health [6]. Breathing air with a high nitrogen oxide concentration can irritate the human respiratory system's airways. Short-term exposure can increase respiratory diseases, such as asthma, coughing, wheezing, and difficulty breathing. NO_2 and other NOx species react with other chemicals in the air to form ozone, which is harmful when inhaled due to its effects on the respiratory system. NOx interacts with the atmosphere's water, oxygen, and other chemicals to form acid rain. Acid rain has a negative impact on sensitive ecosystems, such as lakes and forests. The presence of nitrogen oxides in the atmosphere adds to nutrient contamination in coastal waters.

Because NOx pollution has such a negative impact on the environment and human health, it must be strictly controlled. This involves the implementation of cost-effective removal strategies that simultaneously create value-added by-products or energy from the waste. NOx emissions from various industrial activities and transportation operations, especially coal-fired energy plants, are widely acknowledged as hazards to the environment and human well-being [7]. Since combustion process control can significantly reduce NOx emissions, the treatment of exhaust gases from post-combustion is essential to meet today's statutory air standards [8]. New post-combustion control technologies, such as biotrickling filters (BTFs), could be used to purify NOx-containing dilute gases [9,10].

According to Ligy and Marc], within a biotrickling filter, nitrogen oxide is converted to nitrogen gas under anoxic conditions by chemolithoautotrophic organisms [11]. To resolve this problem, a small number of researchers have worked on isolating thermophilic microorganisms to remove NOx, which may offer greater savings and significantly expand the application of BTFs. Jiang et al. [12] described an effective biotrickling filter system for removing nitric oxide from flue gas using Pseudomonas putida. Liang et al. [13] designed a mathematical model for the elimination of nitric oxide in a thermophilic biotrickling filter. No comprehensive analytical expressions of the nitric oxide concentration in the gas or biofilm phases have been published yet.

Flanagan and Lee [14,15] investigated the reduction of NO by using thermophilic microorganisms at various temperatures. Furthermore, due to the non-linear nature of mass balance equations over the biofilm phase, theoretical modelling studies on NO removal in BTF reactors are limited. Caceres, Song, and Zarook developed theoretical BTF modelling for the removal of volatile organic compounds [16–18]. Under thermophilic circumstances, Liang et al. [13] developed a mathematical model for nitrogen oxide removal in a biotrickling filter. Meena et al. [19,20] discussed mathematical models of the biofiltration of mixtures of hydrophilic (methanol) and hydrophobic (α-pinene) volatile organic compounds (VOCs) in biofilters.

However, to the best of our knowledge, no exact analytical expressions of the nitrogen oxide concentration in the gas and biofilm phases have been reported [13]. The aim of this study is to generate approximate analytical results for the nitrogen oxide concentration in both the gas and biofilm phases using Akbari–Ganji's method. This result will be beneficial in optimizing the key parameters for the efficiency of nitrogen oxide removal from air pollutants by biotrickling filters.

2. Mathematical Formulation of the Problem

A theoretical model of a modern BTF reactor packed with homogenous ceramic particles will now be discussed. This is based on the work reported initially by Liang and co-workers [13]. We briefly describe the principles of a typical experimental biotrickling filter system (refer to Figure 1 of [13]) in order to place the mathematical model in context [13]. Typically, a mass flow controller is used to control the flow of NO, N_2, and O_2 in the experiment with continuous gas streams for the thermophilic removal of NO. A flue gas analyser is used to measure the entry and exit amounts of NO, NO_2, and O_2. The water flow rate through the flow cells is controlled by recirculating the water by means of recirculation pumps. No free liquid is recirculated through the packing materials, and the nutrient liquid is continuously supplied using a top sprayer to minimize the effect of nutrient limitation on biofilm growth. A top sprayer is used to continuously provide the nutrient liquid. As a result, the total BTF operations can be considered in two phases: gas and biofilm, which are connected by a thin interfacial film.

The following assumptions must be included to develop the mass balance equations for both phases [21,22]:

1. The biofilm can be perceived as a planar surface owing to the radius of the packing particles, which is comparatively larger than the biofilm's thickness; the gas flows through the crammed layer in a parallel pattern through a series of vertical channels;
2. The gas phase is moved in a plug flow manner, with no consideration for axial diffusion. Molecule diffusion is used to transport NO in biofilms;
3. The rate-limiting substrate is NO. Therefore, there is no depletion of oxygen or nutrients. It has been proven that the amount of oxygen in the environment is considered in excess, and hence the reaction of NO and molecular oxygen is pseudo-second-order in terms of the NO concentration;
4. The consistent properties of the biofilm across the reactor and negligible biomass production in the packing materials result in a stable value of the biofilm kinetic constants. Here, the biofilm growth is depicted by Monod growth kinetics;
5. Inside the biofilm, only one direction of diffusion/reaction occurs, which is perpendicular to the gas–biofilm boundary. Oxygen in the gas phase influences the partial oxidation of NO to NO_2 and swiftly forms nitrates or nitrates by dissolving in water;
6. Because of oxygen in the gas phase, NO is partially oxidized to NO_2 and quickly dissolved in water to yield nitrite or nitrate. This portion of nitric oxide that has been converted to aqueous nitrogen compounds will not return to the gas phase, so it can be considered to be removed from the gas phase. In fact, nitrite or nitrate in water could be rapidly denitrified to N_2 by denitrifiers.

In Figure 1, we present a schematic representation of the concentration profile of NO_x in the gas and biofilm phases indicating the coordinate systems used and their relation to one another. The concentration profiles refer to a single particle in the biofilter covered with a uniform layer of biofilm of thickness L_f.

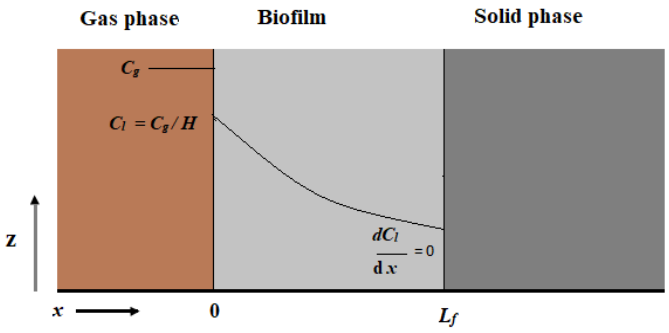

Figure 1. Schematic representation of the NOx concentration distributions in the gas and biofilm phases.

2.1. Mass Balance in the Gas Phase

On the basis of the above assumptions, the mass balance equations in the gas and biofilm phase are given as follows.

$$U_g \frac{dC_g}{dz} = -J_{f,o} a_f - r_c \varepsilon_f \tag{1}$$

where $J_{f,0}$ represents the diffusion flux at the position where $x = 0$, i.e., the flux across the gas/biofilm interface (unit: gcm^{-2} s^{-1}). Furthermore, a_f denotes the specific surface area (surface area/mass) of the biofilm (unit: cm^{-1}), and r_c denotes the gaseous chemical reaction velocity (unit: g cm^{-3} s^{-1}). Noting assumption 6, this gas-phase reaction of NO with molecular oxygen involves the process $2NO + O_2 \rightarrow 2NO_2$, which is rate-determining, and so the rate term is bimolecular and of the type $r_c = 2k_g {C_g}^2$, where we have assumed that oxygen is present in great excess. According to the Fick law, the diffusion flux is related to the concentration gradient at the gas/biofilm interface by the following expression:

$$J_{f,0} = -D_e \left(\frac{dC_\ell}{dx} \right)_{x=0} \tag{2}$$

Hence, the mass balance at x = 0 transforms to:

$$U_g \frac{dC_g}{dz} = a_f D_e \left(\frac{dC_\ell}{dx} \right)_{x=0} - 2k_g {C_g}^2 \tag{3}$$

Note that the initial condition governing this differential equation is given by

$$z = 0 \; C_g = C_{g,0} \tag{4}$$

where C_g and C_l stand for the gas and biofilm phase NO concentrations, U_g is the superficial gas velocity, a_f is the surface area of biofilm, D_e denotes the effective diffusion coefficient of NO within the biofilm phase, k_g is the bimolecular reaction rate constant, and ε_f denotes the biofilm porosity ratio. We note that x represents the coordinate axis calculated from the surface of the biofilm and whose direction is perpendicular to the surface of the biofilm-coated particle. Furthermore, we note that the variable z denotes the height from the bottom of the packing materials and so defines a coordinate representing the length of the biofiltration column.

2.2. Mass Balance Equation in the Biofilm Phase

The expression for the mass balance in the biofilm phase is given by the balance between the molecular diffusion of NO through the liquid phase and the reaction kinetics by which the NO substrate of concentration C_ℓ is transformed by immobilized microorganisms according to Monod kinetics:

$$D_e \frac{d^2 C_\ell}{dx^2} = \frac{\mu_m}{Y} \frac{C_\ell}{K_S + C_\ell} X_V \tag{5}$$

where μ_m is the maximum specific biomass growth rate, Y is the yield coefficient of microorganisms, μ_m / Y gives the maximum specific substrate utilization rate, K_S is the Monod half-saturation constant, X_V is the biofilm microbial density, H is Henry constant at a fixed temperature, and L_f is the biofilm thickness.

The boundary conditions governing the reaction diffusion equation in the biofilm are given by

$$\text{At} \quad x = 0, \;\; C_\ell(x = 0) = \frac{C_g}{H} \tag{6}$$

$$\text{At} \quad x = L_F, \;\; \frac{dC_\ell}{dx} = 0 \tag{7}$$

The first boundary condition specifies the partitioning of the NO species from the gas phase to the liquid biofilm and H represents the gas/liquid Henry volatility constant for temperature T. This value decreases as the gas solubility increases. The second condition relates to a zero-flux condition and the biofilm/solid particulate support interface, since the support particle is assumed to be inert.

2.3. Dimensionless Form

The problem may be expressed in an efficient format by defining the following dimensionless parameters that involve scaling the NO concentration and introducing normalized distance parameters, a saturation parameter, a reaction/diffusion parameter, and parameters comparing molecular diffusion with gas velocity and gas-phase chemical reaction with the superficial gas velocity, as follows:

$$C_\ell(x) = \frac{C_\ell}{C_{g/H}}, \quad x = \frac{x}{L_F}\ \alpha = L_F\sqrt{\frac{\mu_m X_V}{YD_eK_S}}, \ \beta = \frac{C_{g/H}}{K_S} \tag{8}$$

$$C_g(z) = \frac{C_g(z)}{C_{g,0}}, \ z = \frac{z}{L_F}, \quad \gamma = \frac{a_F D_e}{U_g H}, \quad \eta = \frac{\varepsilon_f k_g C_{g,0} L_F}{U_g} \tag{9}$$

We can readily show that Equation (5) reduces to the following normalized form with the corresponding boundary conditions as follows:

$$\frac{d^2C_\ell}{dx^2} - \frac{\alpha^2 C_\ell}{1+\beta C_\ell} = 0 \tag{10}$$

$$C_\ell(x=0) = 1 \tag{11}$$

$$\left(\frac{dC_\ell}{dx}\right)_{x=1} = 0 \tag{12}$$

Note that Equation (10) is a non-linear differential equation describing molecular diffusion and Monod kinetics within the thin biofilm. We assume that the biofilm thickness is much smaller than the radius of the support particle, and so the geometry of the reaction/diffusion problem is assumed to be planar without serious error. Furthermore, Equation (1) describing the mass balance at the gas/biofilm phase boundary is converted to the normalized form as shown below:

$$\frac{dC_g}{dz} - \gamma C_g\left(\frac{dC_\ell}{dx}\right)_{x=0} + 2\eta {C_g}^2 = 0 \tag{13}$$

$$C_g(z=0) = 1 \tag{14}$$

We note that Equation (10) is nonlinear. As outlined in Appendix A, we show that this non-linear first-order differential equation for the NO concentration in the gas phase is of the Bernoulli type and may be transformed into a first-order linear differential equation by means of a simple substitution. We now discuss how an efficient approximate analytical solution to these coupled nonlinear differential equations may be solved using the Akbari–Ganji method (AGM).

3. Approximate Analytical Expression of the Concentration Using the Akbari–Ganji Method

Nowadays, many analytical methods are available for solving nonlinear differential equations [23–31]. Such methods include the Akbari–Ganji method [32–35], domain decomposition method [36,37], homotopy perturbation method [38–41], Taylor's series method [42–44], variational iteration method [45], and Padé approximant method [46].

One of the most successful methods for solving nonlinear differential equations is the AGM method. AGM has a very simple approach to solving a differential equation as compared with other semi-analytical techniques, requiring only the initial/boundary conditions, the main differential equations, and their derivatives. In this study, this method is used for the first time to derive analytical expressions for the NO concentration both in the gas and biofilm phases of a biotrickling filter.

As presented in Appendix A, we can show that the Akbari–Ganji technique can be used to derive an analytical expression for the NO concentration in the biofilm phase $\overline{C_l}(\overline{x})$ for all values of the dimensionless reaction/diffusion parameter α and the binding/saturation parameter β as follows:

$$\overline{C}_\ell(\overline{x}) = \frac{\cosh\left[\frac{\alpha}{\sqrt{1+\beta}}(1-\overline{x})\right]}{\cosh\left[\frac{\alpha}{\sqrt{1+\beta}}\right]} = \operatorname{sech}\left[\frac{\alpha}{\sqrt{1+\beta}}\right]\cosh\left[\frac{\alpha}{\sqrt{1+\beta}}(1-\overline{x})\right] \tag{15}$$

Furthermore, we show in Appendix B that an analytical expression for the NO concentration in the gas phase is given by the following expression:

$$C_g(z) = n\{(\exp[nz](n+2\eta)) - 2\eta\}^{-1} \tag{16}$$

where the parameter n is related to the flux of NO through the biofilm and is given by the following expression:

$$n = -\gamma C_\ell^{'}(x=0) \tag{17}$$

Furthermore, we note that the differentiation of Equation (15) enables us to compute a simple closed-form value for the NO flux in the biofilm phase, which is given by:

$$J_0 = -\left(\frac{d\overline{C}_\ell(\overline{x})}{d\overline{x}}\right)_{\overline{x}=0} = \frac{\alpha}{\sqrt{1+\beta}}\tanh\left[\frac{\alpha}{\sqrt{1+\beta}}\right] \tag{18}$$

This expression for the flux of NO through the biofilm can be related in a simple manner to the degree of saturation of Monod kinetics in the film and the rate of molecular diffusion to NO utilization by the immobilized microbe species in the layer. From Equations (17) and (18), we can show that:

$$n = \frac{\alpha\gamma}{\sqrt{1+\beta}}\tanh\left[\frac{\alpha}{\sqrt{1+\beta}}\right] \tag{19}$$

Hence, Equations (14) and (15) define the desired relation between the concentration of NO in the gas phase and the flux of NO in the biofilm phase. From Equations (10) and (13), we obtain the following expression for the NO concentration in the gas phase:

$$C_g(z) = \frac{\frac{\alpha\gamma}{\sqrt{1+\beta}}\tanh\left[\frac{\alpha}{\sqrt{1+\beta}}\right]}{\exp\left(\frac{\alpha\gamma}{\sqrt{1+\beta}}\tanh\left[\frac{\alpha}{\sqrt{1+\beta}}\right]z\right)\left(\frac{\alpha\gamma}{\sqrt{1+\beta}}\tanh\left[\frac{\alpha}{\sqrt{1+\beta}}\right]+2\eta\right)-2\eta} \tag{20}$$

Hence, we have derived two closed-form expressions for the NO concentration in both the gas and biofilm phases that are in good agreement with the numerical solution over a wide range of parameters, as indicated later in this paper.

4. Removal Efficiency of Nitric Oxide

The NO absorption ratio or NO removal efficiency is expressed as follows [42]:

$$RE = \frac{[\mathrm{NO}]_i - [\mathrm{NO}]_f}{[\mathrm{NO}]_i} = 1 - \frac{[\mathrm{NO}]_f}{[\mathrm{NO}]_i} = 1 - \frac{\overline{C}_g(\overline{z})}{[\mathrm{NO}]_i} \tag{21}$$

where NO_i and NO_f represent the initial (pre-treatment) and the final (post-treatment) NO concentrations in the gas phase.

5. Previous Analytical Results

It is useful to compare the AGM-derived expressions outlined in Equations (15) and (20) for the NO concentration with analytical expressions derived using different methods. Rasi et al. [36] used the Adomian decomposition method (ADM) to solve Equations (10) and (13) with the associated boundary conditions used in the present paper. Their analytical expressions for the NO concentration of the biofilm and gas phases are, respectively, given by

$$C_\ell(x) = 1 - \frac{\alpha^2 x}{2(1+\beta)}\left\{2 - x - \frac{\alpha^2\left(x^2(x-4)+8\right)}{12(1+\beta)^2}\right\} \tag{22}$$

and

$$C_g(z) = \frac{\gamma m}{\exp[\gamma m z](\gamma m + 2\eta) - 2\eta} \tag{23}$$

where

$$m = \frac{\alpha^2}{1+\beta}\left\{\frac{\alpha^2}{3(1+\beta)^2} - 1\right\} \tag{24}$$

These expressions are also very useful for numerical computation.

6. Numerical Simulation

The non-linear reaction/diffusion equation in the biofilm phase outlined in Equation (15) is solved numerically for the relevant boundary conditions. As outlined in Appendix C, the MATLAB function bvp4c is used to solve this equation, which is a function for solving two-point boundary value problems for nonlinear differential equations. These numerical solutions were then compared with the approximate closed-form analytical solutions derived via the AGM to probe the accuracy of the latter.

Consequently, in Table 1 and Figures 2–4, the analytical results for the NO concentration were compared with simulation data and previously available analytical results (obtained using ADM). The maximum average error between our new analytical result (obtained using the AGM method) and the simulation result was 0.64%. In comparison, the previous analytical result (obtained via the ADM method) and the simulation result had a maximum average error of 5.05%. Therefore, we conclude that the ADM method has a prolonged convergence rate and the AGM provides a better fit for simulation predictions. The AGM method is also attractive since it enables the development of a closed-form analytical solution to a non-linear reaction/diffusion equation that can be computed readily, and can be readily interpreted in terms of the degree of utilization of the biofilm in the consumption of the target substrate.

Table 1. Comparison between numerical and analytical results for the dimensionless NO concentration of the biofilm phase $\bar{c}_l(\bar{x})$ for various values of parameter α when $\beta = 0.01$.

$\bar{x}$	α = 0.01					α = 0.5					α = 1				
		Concentration in Biofim Phase		Error (%)			Concentration in Biofim Phase		Error (%)			Concentration in Biofim Phase		Error (%)	
	Num.	This Work AGM Equation (15)	ADM [31] Equation (22)	This Work AGM Equation (15)	ADM [31] Equation (22)	Num.	This Work AGM Equation (15)	ADM [31] Equation (22)	This Work AGM Equation (15)	ADM [31] Equation (22)	Num.	This Work AGM Equation (15)	ADM [31] Equation (22)	AGM Equation (15)	ADM [31] Equation (22)
0	1.0000	1.0000	1.0000	0.00	0.00	1.0000	1.0000	1.0000	0.00	0.00	1.0000	1.0000	1.0000	0.00	0.00
0.2	0.9982	0.9982	0.9982	0.00	0.00	0.9587	0.9587	0.9591	0.00	0.04	0.8663	0.8666	0.8843	0.03	2.07
0.4	0.9968	0.9968	0.9968	0.00	0.00	0.9271	0.9271	0.9278	0.00	0.08	0.7678	0.7683	0.8019	0.06	4.44
0.6	0.9958	0.9958	0.9958	0.00	0.00	0.9049	0.9049	0.9058	0.00	0.09	0.7005	0.7011	0.7473	0.08	6.68
0.8	0.9953	0.9953	0.9953	0.00	0.00	0.8918	0.8918	0.8929	0.01	0.12	0.6617	0.6624	0.7165	0.11	8.28
1	0.9951	0.9951	0.9951	0.00	0.00	0.8877	0.8877	0.8889	0.01	0.13	0.6498	0.6605	0.7072	0.11	8.83
	Average error %			0.00	0.00	Average error %			0.01	0.08	Average error %			0.06	5.05

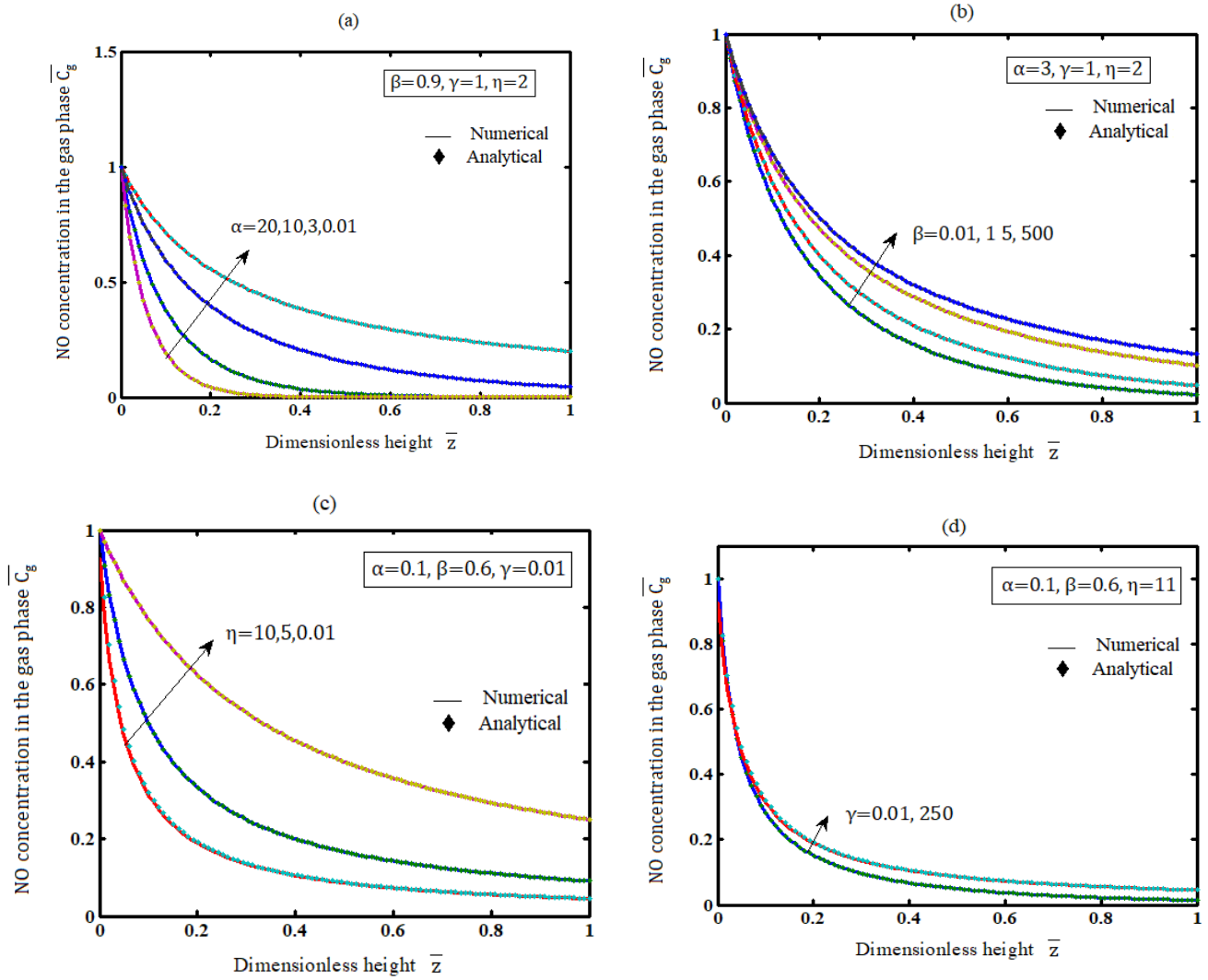

Figure 2. Dimensionless NO concentration in the gas phase using Equation (20) for the experimental values (Table A1)of the parameters (**a**) α. (**b**) β. (**c**) η. (**d**) γ.

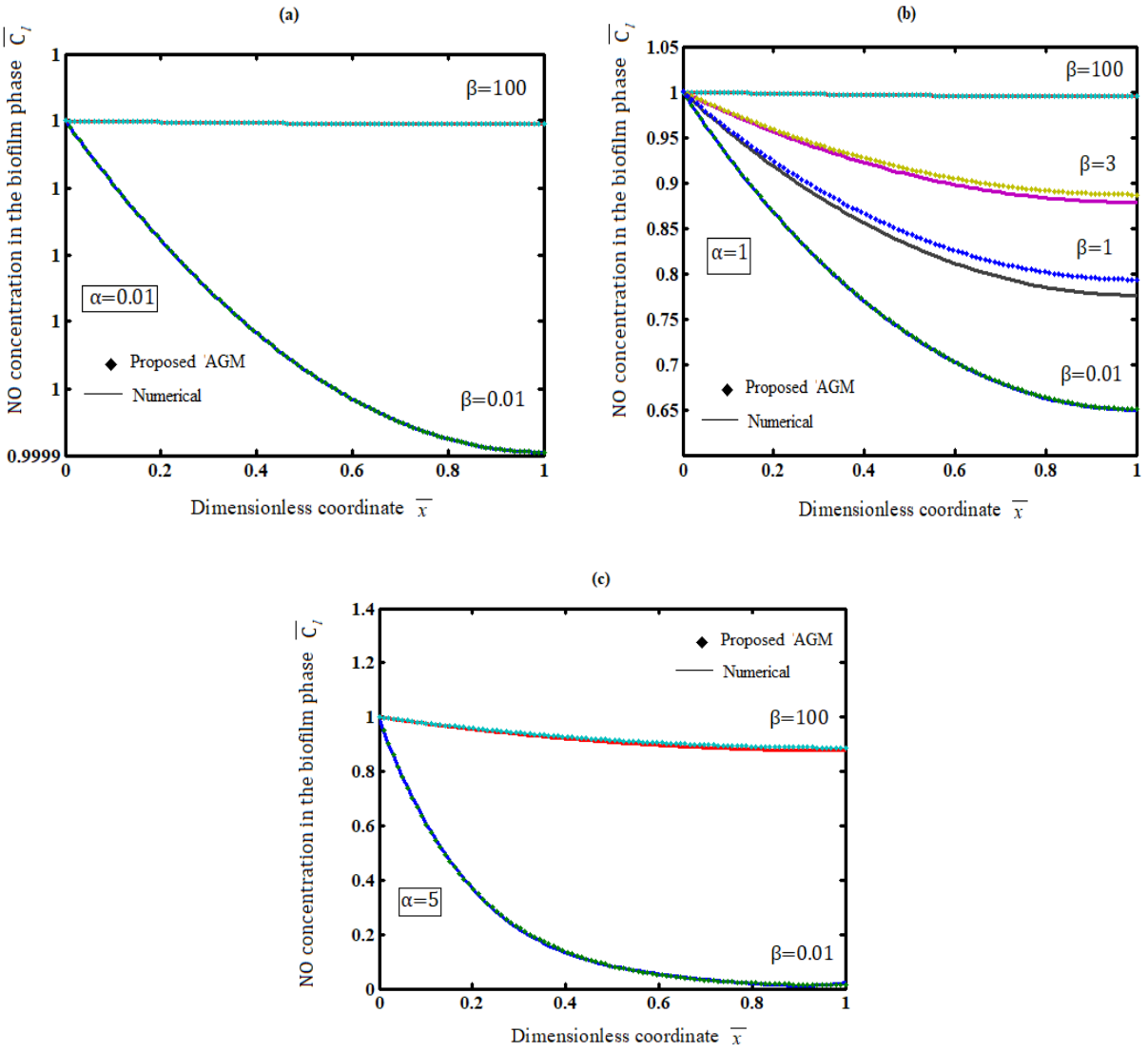

Figure 3. Dimensionless NO concentration in the biofilm phase $\overline{C_l}$ computed using Equation (15) for various experimental (Table A2) values of β (when (**a**) $\alpha = 0.01$ (**b**) $\alpha = 1$ (**c**) $\alpha = 5$.

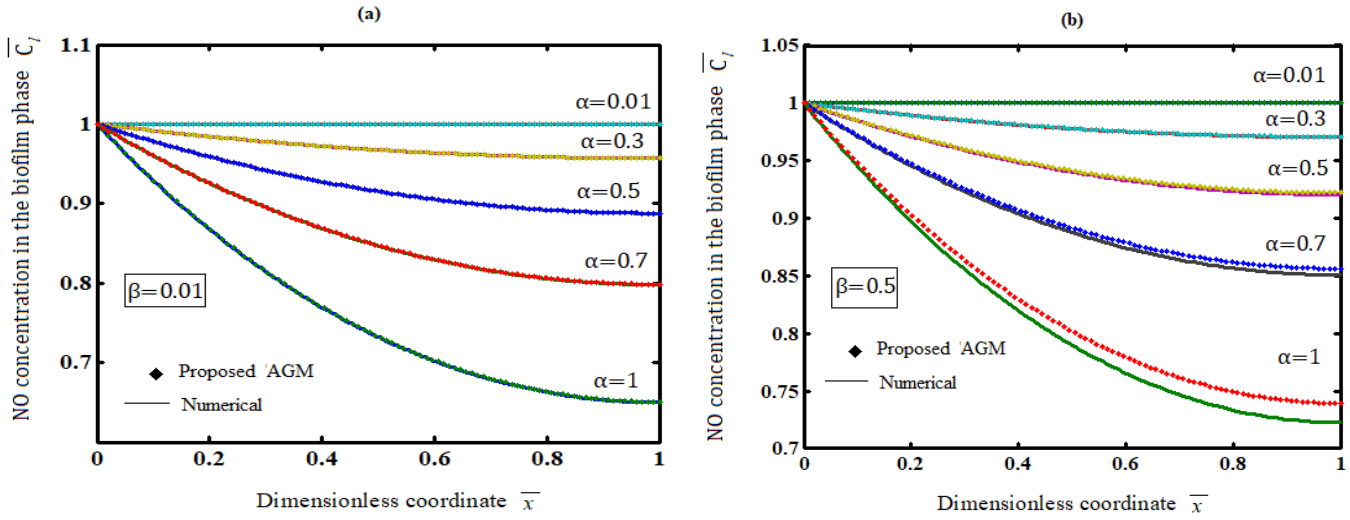

Figure 4. *Cont.*

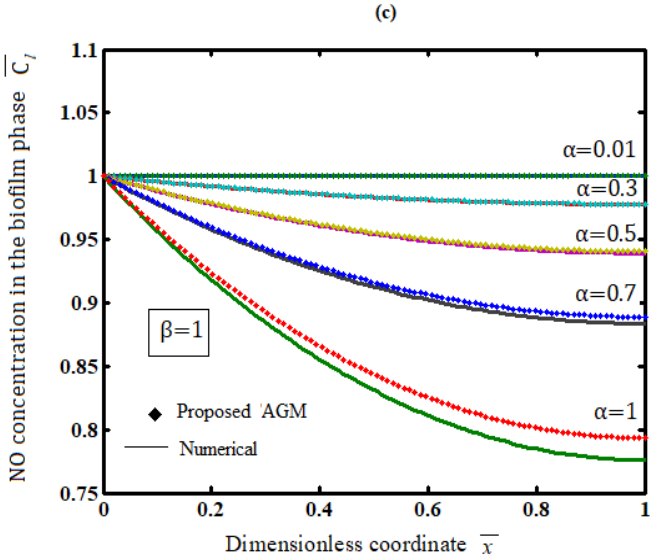

Figure 4. Dimensionless NO concentration in the biofilm phase $\overline{C_l}$ computed using Equation (15) for various experimental values of α and β (Table A2) when (**a**) $\beta = 0.01$ (**b**) $\beta = 0.5$ (**c**) $\beta = 1$.

7. Results and Discussion

We note that Equations (15) and (20) defined the AGM-based approximate analytical expressions for the NO concentration in the biofilm and gas phases, which were valid for all experimental values of the parameters α, $\beta, \gamma,$ and η. The parameters α and η scaled with the biofilm thickness L_f. Note that β is the inlet NO concentration. Additionally, we note that $\gamma \left(= \frac{a_f D_e}{H U_g}\right)$ was proportional to the specific area of the biofilm a_f and the effective diffusion coefficient D_e, and was inversely proportional to the Henry coefficient H and the superficial gas velocity U_g.

The effects that the various parameters α, $\gamma,$ and η had on the NO concentration profiles are shown in Figure 2a–d. A decrease in all parameters led to a decrease in the concentration of NO in the gas phase $\overline{C_g}$. As the standardized parameter β increased, the gas-phase NO concentration $\overline{C_g}$ increased and reached its maximum value when dimensionless height $\overline{z} = 0$.

We note that Figure 3a–c represents the concentration profiles of NO in the biofilm phase $\overline{C_l}$ computed via the AGM-based expression defined in Equation (8) for different values of the parameters, as indicated. From Figure 3a–c, it can be inferred that the concentration of NO in the biofilm phase $\overline{C_l}$ increases when β increases for different values of α. The NO concentration of the biofilm phase reached its maximum when $\alpha < 0.01$ and $\beta \geq 100$.

Figure 4a–c shows the effect of parameter α on the concentration of NO in the biofilm phase. From the Figures, it was inferred that the concentration of NO decreased when increasing the parameter α.

To evaluate the biotrickling filter performance, one should consider the maximum removal efficiency. The reactor design for an industrial application often needs to achieve a high removal percentage. Figure 5 represents the NO removal ratio versus the dimensionless height for various experimental values of the parameters (Table A2). As indicated in Figure 5, the maximum removal efficiency was reduced accordingly if the inlet concentration was very low. This mathematical procedure can be applied for the removal of volatile organic compounds from air [47–51]. Additionally, this method can be extended for the removal of sulfur dioxide, nitric oxide [52], by the chemical absorption–biological reduction integrated process [6].

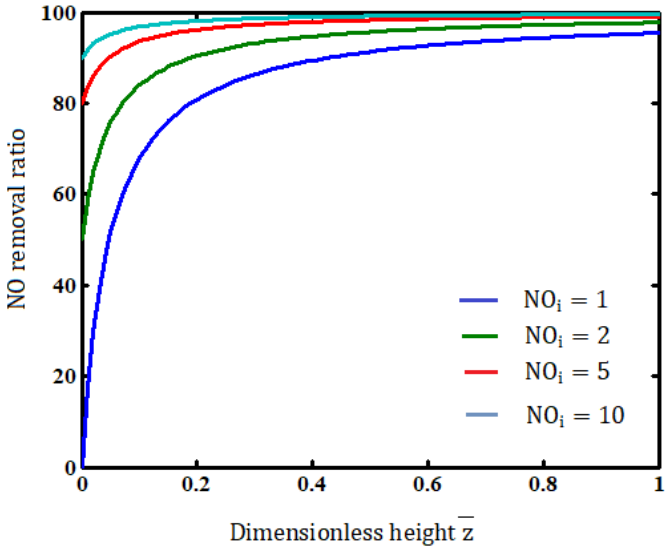

Figure 5. NOx removal T ratio NO_R for various values of NO_i. The experimental values of parameter [8] (Appendix C) are $\alpha = 0.1121$, $\beta = 0.629$, $\gamma = 0.0126$, and $\eta = 10.5$, according to Equation (21).

Limitation of This Model

Biofilms are formed when microorganisms adhere to surfaces. Because of their function in certain infectious diseases and their importance in many device-related infections, biofilms are extremely important for public health. The term biofilm is sometimes a misnomer, since biofilms are not continuous monolayer surface deposits. Instead, biofilms are highly heterogeneous, containing microcolonies of bacterial cells encased in an EPS matrix and separated from other microcolonies. However, in our model, the assumption about vertical channel, no axial diffusion, and homogeneity in a biofilm are in contrast with the real heterogeneous nature of biofilms.

A fundamental property believed to influence biofilms' community structures is biofilm thickness. However, since biofilm thickness is inextricably linked to external factors, such as water flow, temperature, development age, and nutrient conditions, its importance is difficult to quantify. Biofilm thickness varies depending on the species, substrate, time required for maturation, and microenvironment conditions, such as nutrient availability and shear flow. Its thickness also depends on the linear velocity $L_f = f(t)$; the higher the velocity, the thinner the boundary layer. However, in our steady-state model under oligotrophic conditions, we assume that the thickness of the biofilm is constant. This is another limitation of this model.

Biofilms are composed primarily of microbial cells and EPS. EPS can comprise 50% to 90% of the total organic carbon in biofilms and can be considered the primary matrix material of the biofilm. EPS may vary in terms of the nitric oxide diffusion and conversion rates (chemical and physical properties). However, we assumed that the gas phase is moved in a plug flow manner in our model, with no consideration for axial diffusion.

In this paper, a thermophilic biotrickling filter (BTF) system was discussed to inoculate a newly isolated strain of Chelatococcus daeguensis TAD1 for the effective treatment of nitrogen oxide. However, many systems are essentially open, and the observed biofilms always contain a variety of microbial species (e.g., bacteria, fungi, and higher organisms). Our method can also be extended to other microbial species.

8. Conclusions

In this paper, a mathematical model of NOx removal in the gas and biofilm phases of a biotrickling filter is solved to produce an analytical expression for the NO concentration using the Akbari–Ganji method, which has been shown to be effective and reliable. The approximate analytical expression of the NOx concentration in the gas and biofilm phases

for all experimental values of the parameters is derived. A satisfactory agreement is noted between the obtained analytical results and the existing numerical results, and indeed with previous approximate solutions. The influence of the biofilm thickness and inflow concentration can be studied using these analytical expressions.

Based on our mathematical expression of the removal efficiency, the optimal parameters of the device could be determined and adjusted in advance to achieve the maximum nitrogen oxide removal efficiency using a biotrickling filter. This type of analysis the biotrickling filter (BTF) model can be used to remove styrene from airstreams, large loads of hydrogen sulphide from biogas streams, and volatile organic compounds from contaminated air.

Author Contributions: Conceptualization, M.E.G.L. and L.R.; methodology, M.E.G.L.; software, R.U. and P.J.; validation, L.R. and K.V.; formal analysis, L.R.; investigation, M.E.G.L.; resources, R.U.; data curation, K.V.; writing—original draft preparation, P.J.; writing—review and editing, L.R.; visualization, P.J.; supervision, M.E.G.L. and L.R.; project administration, M.E.G.L. All authors have read and agreed to the published version of the manuscript.

Funding: This research received no external funding.

Institutional Review Board Statement: Not applicable.

Informed Consent Statement: Not applicable.

Acknowledgments: The authors are thankful to the reviewers for their valuable comments. They express their gratitude to Shri J. Ramachandran, Chancellor, G. Thiruvasagam, Vice-Chancellor and M. Jayaprakashvel, Registrar, Academy of Maritime Education and Training (AMET), Chennai, Tamil Nadu, for their continuous encouragement.

Conflicts of Interest: The authors declare no conflict of interest.

Nomenclature

Symbols	Description	Units
a_f	Specific surface area of the biofilm	cm^{-1}
$a0$	Specific surface area of the medium	cm^{-1}
Cg	NO concentration in the gas phase	g cm^{-3}
C_l	NO concentration in the biofilm phase	g cm^{-3}
$C_{g,0}$	Inlet NO concentration	g cm^{-3}
$\overline{C_g}$	Dimensionless NO concentration in the gas phase	None
$\overline{C_l}$	Dimensionless NO concentration in the biofilm phase	None
D_e	Effective diffusion coefficient in the biofilm	cm^2 s^{-1}
H	Henry constant	None
K_S	Monod half-saturation constant	g cm^{-3}
k_g	Reaction rate constant	cm^3 g^{-1} s^{-1}
L_f	Biofilm thickness	cm
NO_i	Initial NO concentration in the gas phase	None
NO_f	Final NO concentration in the gas phase	None
NO_R	NO removal ratio (NO removal efficiency)	None
U_g	Superficial gas velocity	cm s^{-1}
X_V	Microbial density of the biofilm	g cm^{-3}
x	Coordinate axis calculated from the surface of the biofilm	cm
$\overline{x}$	Dimensionless height calculated from the base of the packing material	None
Y	Yield coefficient of microorganisms	g_b/g_i
z	Height value calculated from the base of the packing materials	cm
$\overline{z}$	Dimensionless parameter	None
μ	Growth rate of biomass	s^{-1}
μ_m	Maximum specific growth rate of biomass	s^{-1}
ε_f	Porosity ratio of biofilm-covered packing materials	None
ε_0	Porosity of medium	None
α, β, γ, η	Dimensionless parameters	None

Appendix A. Analytical Expression of Concentration of Biofilm and Gas Phase

To employ the Akbari–Ganji method (AGM), assume that the solution to Equation (7) is of the following hyperbolic form:

$$\overline{C}_\ell(\overline{x}) = A_0 \cosh[m\overline{x}] + B_0 \sinh[m\overline{x}] \tag{A1}$$

where A_0, B_0, and m are constants. From boundary conditions (8) and (9), the values of A_0 and B_0 are readily obtained, that is:

$$A_0 = 1 \; B_0 = -\tanh[m] \tag{A2}$$

Hence, Equation (A1) becomes, after some algebra,

$$\overline{C}_\ell(\overline{x}) = \frac{\cosh[m(1-\overline{x})]}{\cosh[m]} \tag{A3}$$

To determine the constant m in Equation (A3), we consider the functional form of Equation (7) as follows:

$$F(\overline{x}) = \left(1 + \beta \overline{C}_\ell(\overline{x})\right) \frac{d^2\overline{C}_\ell(\overline{x})}{d\overline{x}^2} - \alpha^2 \overline{C}_\ell(\overline{x}) = 0 \tag{A4}$$

By substituting Equation (A3) into Equation (A4), we obtain:

$$F(\overline{x})|_{\overline{x}=0} = \left(1 + \frac{\beta \cosh[m]}{\cosh[m]}\right) \frac{m^2 \cosh[m]}{\cosh[m]} = \alpha^2 \tag{A5}$$

From the above equation, we get the following useful result for *m:*

$$m = \pm \frac{\alpha}{\sqrt{1+\beta}} \tag{A6}$$

Substituting Equation (A7) into Equation (A3) gives the following analytical expression of the concentration of biofilm phase $\overline{C_l}(\overline{x})$ for all dimensionless parameters α and β.

$$\overline{C}_\ell(\overline{x}) = \operatorname{sech}\left[\frac{\alpha}{\sqrt{1+\beta}}\right] \cosh\left[\frac{\alpha}{\sqrt{1+\beta}}(1-\overline{x})\right] \tag{A7}$$

We also note that the flux of NO in the biofilm phase is given by the following expression.

$$\overline{C}'_\ell(\overline{x}=0) = -\left(\frac{d\overline{C}_\ell}{d\overline{x}}\right)_{\overline{x}=0} = \frac{\alpha}{\sqrt{1+\beta}} \tanh\left[\frac{\alpha}{1+\beta}\right] \tag{A8}$$

Now noting Equation (17) in the main text, we can obtain the following assignment for parameter n as follows:

$$n = -\gamma\left(\frac{dC_\ell(\overline{x})}{dx}\right)_{x=0} = \frac{\alpha\gamma}{\sqrt{1+\beta}} \tanh\left[\frac{\alpha}{\sqrt{1+\beta}}\right] \tag{A9}$$

Using the transformed Equation (13) for the mass balance at the gas/biofilm interface introduced in Equation (13) in the main text,

$$\begin{array}{c} \frac{d\overline{C}_g}{d\overline{z}} - \gamma \overline{C}_g \left(\frac{d\overline{C}_\ell}{d\overline{x}}\right)_{\overline{x}=0} + 2\eta {\overline{C}_g}^2 = 0 \\ \overline{C}_g(\overline{z}=0) = 1 \end{array} \tag{A10}$$

Noting Equations (17) and (19) in the main text and Equation (A11), we can readily show that the governing equation governing the variation in the NO concentration with distance in the gas phase (Equation (13) in the main text) can be written as

$$\frac{d\overline{C}_g}{d\overline{z}} + n\overline{C}_g + 2\eta\overline{C}_g{}^2 = 0 \tag{A11}$$

We note that Equation (A13) is non-linear. We note, however, that this nonlinear equation can be transformed via a standard textbook substitution into a linear Bernoulli-type differential equation, which can be readily integrated using the separation of variables (Table A1). Noting the pertinent initial condition that $\overline{C}(\overline{z} = 0) = 1$, we can show that the analytical expression for the concentration of NO species in the gas phase is given by:

$$\overline{C}_g(\overline{z}) = \frac{n}{\exp[n\overline{z}](n + 2\eta) - 2\eta} = \frac{n}{n\exp[n\overline{z}] + 2\eta(\exp[n\overline{z}] - 1)} \tag{A12}$$

This is the expression for the concentration of NO in the gas phase presented in Equation (20) in the main body of the paper.

Appendix B. Solution of Bernulli Type Equations

The non-linear Bernoulli differential equation admits the following form:

$$\frac{dy}{dx} + p(x)y = q(x)y^m \; m \neq 0, 1 \tag{A13}$$

When $m = 0, 1$ the differential equation becomes linear. We assume, for simplicity, that both *P(x)* = *p* and *q(x)* = *q* = *constant*, and so Equation (A13) simplifies to:

$$\frac{dy}{dx} + py = qy^m \tag{A14}$$

We use the following substitution $v = y^{1-m}$ in Equation (A14) to transform to a linear expression. Dividing across Equation (A14) by y^m, we obtain

$$\frac{1}{y^m}\frac{dy}{dx} + py^{1-m} = q \tag{A15}$$

We note that $\frac{dy}{dx} = \frac{dv}{dx}.\frac{dy}{dv}$, hence, $\frac{dv}{dx} = \frac{d}{dx}(y^{1-m}) = \frac{dv}{dy}\frac{dy}{dx} = (1-m)y^{-m}\frac{dy}{dx}$. Hence, we note that $\frac{dy}{dx} = \frac{y^m}{(1-m)}\frac{dv}{dx}$, and so $\frac{1}{y^m}\frac{dy}{dx} = \frac{1}{(1-m)}\frac{dv}{dx}$, and so the non-linear expression outlined in Equation (A15) takes the general form:

$$\frac{dv}{dx} + (1-m)pv = (1-m)q \tag{A16}$$

The current problem demands that we set *m* = 2; hence, Equation (A16) becomes:

$$\frac{dv}{dx} = pv - q \tag{A17}$$

This expression may now be readily solved via the separation of variables as follows: $\frac{dv}{pv-q} = dx$. Setting $u = -q + pv$, we get $dv = \frac{du}{p}$ and we note that: $\frac{du}{u} = pdx$.

Integrating: $\frac{du}{u} = pdx$, we obtain $\frac{1}{p}\ln u = x + K$ or $\frac{1}{p}\ln(pv - q) = x + K$. When $x = 0$, $v = 1$, so the constant of integration is given by $K = \frac{1}{p}\ln(p - q)$. Hence, Equation (A17) integrates to:

$$\frac{1}{p}\ln(pv - q) = x + \frac{1}{p}\ln(p - q) \tag{A18}$$

We can readily show that Equation (A18) reduces to:

$$\frac{pv - q}{p - q} = \exp[px] \tag{A19}$$

Finally, solving for $v(x)$ produces:

$$v(x) = \frac{q}{p} + \left(1 - \frac{q}{p}\right)\exp[px] \tag{A20}$$

When $x = 0$, $v(x) = v_0 = 1$, and so $v(x = 0) = \frac{q}{p} + (1 - \frac{q}{p}) = 1$, and the solution obeys the initial condition. Hence, Equation (A20) is a proper solution of the differential equation. Finally, noting that $y = 1/v$, Equation (A20) takes the following form:

$$y(x) = \frac{1}{\frac{q}{p} + (1 - \frac{q}{p})\exp[px]} = \frac{p}{q + p(1 - \frac{q}{p})\exp[px]} \tag{A21}$$

Note that Equation (A21) is of the same form as that provided in the main body of the paper or in Appendix A (Equation (A12)), provided we assign $p = n$, $q = -2\eta$, and $y = \overline{C}_g(\overline{z})$.

Table A1. Experimental Value of the Parameters [13] Used in This Work (Figure 5).

Symbols	Description	Units	Experimental Values
ε_0	Porosity of the medium	None	0.62
a_0	Specific surface area of the medium	m^{-1}	398
D_e	Effective diffusion coefficient in the biofilm	$cm^2\ s^{-1}$	5.21×10^{-5}
L_f	Biofilm thickness	cm	0.1
$L = \frac{2\varepsilon_0}{a_0}$	Characteristic length of the vertical channels	m	0.003
k_g	Reaction rate constant	$L^2\ mol^{-2}\ s^{-1}$	6.496×10^3
K_S	Monod half-saturation constant	$g\ cm^{-3}$	6×10^{-8}
H	Henry constant	None	26.5
X_V	Microbial density of the biofilm	$g\ cm^{-3}$	0.4×10^{-7}
μ_m/Y	Maximum specific substrate utilization rate	s^{-1}	9.8×10^{-5}
U_g	Superficial gas velocity	$cm\ s^{-1}$	0.8 to 2.4
C_g	NO concentration in the gas phase	$g\ cm^{-3}$	10^{-5} to 10^{-6}
$C_{g,0}$	Inlet NO concentration	$g\ cm^{-3}$	5×10^{-5}
$a_f = a_0\left(1 - \frac{L_f}{L}\right)$	Specific surface area of the biofilm	cm^{-1}	12,876.34
$\varepsilon_f = \varepsilon_0\left(1 - \frac{L_f}{L}\right)^2$	Porosity ratio of biofilm-covered packing materials	None	648
$\alpha = L_f\sqrt{\frac{\mu_m X_V}{Y D_e K_S}}$	Dimensionless parameter	None	0.1121
$\beta = \frac{C_g/H}{K_S}$	Dimensionless parameter	None	0.629
$\gamma = \frac{a_f D_e}{H U_g}$	Dimensionless parameter	None	0.0126
$\eta = \frac{\varepsilon_f k_g C_{g,0} L_f}{U_g}$	Dimensionless parameter	None	10.5

Table A2. Experimental Dimensionless Values of the Parameters [13] Used in This Work (Figures 2–4 and Table 1).

Dimensionless Parameter	Experimental Value of Parameters Used in [13]	Value of the Parameter Used in Figures 2–4 and Table 1	Value of the Parameter Used in Figure 5
$\alpha = L_f \sqrt{\frac{\mu_m X_V}{Y D_e K_S}}$	0.1121	0.01 to 20	0.1121
$\beta = \frac{C_g/H}{K_S}$	0.629	0.01 to 500	0.629
$\gamma = \frac{a_f D_e}{H U_g}$	0.0126	0.01 to 250	0.0126
$\eta = \frac{\varepsilon_f k_g C_{g,0} L_f}{U_g}$	10.5	0.01 to 10	10.5

Appendix C. MATLAB Code for the Numerical Solution of the Non-Linear Equation (10)

```
function pdex4
m = 0;
x = linspace(0,1);
t = linspace(0,10);
sol = pdepe(m,@pdex4pde,@pdex4ic,@pdex4bc,x,t);
u1 = sol(:,:,1);
figure
plot(x,u1(end,:))
title('u1(x,t)')
xlabel('Distance x')
ylabel('u1(x,2)')
%——————————————————————————————
function [c,f,s] = pdex4pde(x,t,u,DuDx)
c = [1];
f = [1].* DuDx;
Alpha = 0.5;
Beta = 0.5;
F = −((alpha^2)*u(1))/(1+beta*u(1));
s=[F];
% ——————————————————————————————-
function u0 = pdex4ic(x);
%create a initial conditions
u0 = [1];
% ——————————————————————————————-
function [pl,ql,pr,qr]=pdex4bc(xl,ul,xr,ur,t)
%create a boundary conditions
pl = [ul(1)−1];
ql = [0];
pr = [0];
qr = [1];
```

References

1. Deshusses, M.A.; Shareefdeen, Z. Modeling of Biofilters and Biotrickling Filters for Odor and VOC Control Applications. In *Biotechnology for Odor and Air Pollution Control*; Shareefdeen, Z., Singh, A., Eds.; Springer: Berlin/Heidelberg, Germany, 2005. [CrossRef]
2. Kalantar, M.; Zamir, S.M.; Ferdowsi, M.; Shojaosadati, S.A. Removal of toluene in a biotrickling filter in the presence of methanol vapors: Experimental study, mathematical modeling, and kinetic parameters optimization. *J. Environ. Chem. Eng.* **2021**, *9*, 104617. [CrossRef]
3. San-Valero, P.; Penya-Roja, J.M.; Alvarez-Hornos, F.J.; Marzal, P.; Gabaldón, C. Dynamic mathematical modelling of the removal of hydrophilic vocs by biotrickling filters. *Int. J. Environ. Res. Public Health* **2015**, *12*, 746–766. [CrossRef] [PubMed]
4. Apel, W.A.; Turick, C.E. Use of Denitrifying bacteria for the removal of nitrogen oxides from combustion gases. *Fuel* **1993**, *72*, 1715–1718. [CrossRef]
5. Du Plessis, C.A.; Kinney, K.A.; Schroeder, E.D.; Chang, D.P.Y.; Scow, K.M. Denitrification and nitric oxide reduction in an aerobic toluene-treating biofilter. *Biotechnol. Bioeng.* **1998**, *58*, 408–415. [CrossRef]
6. Zhao, J.; Xia, Y.; Li, M.; Li, S.; Li, W.; Zhang, S. A biophysicochemical model for no removal by the chemical absorption−biological reduction integrated process. *Environ. Sci. Technol.* **2016**, *50*, 8705–8712. [CrossRef]

7. Bogner, W.; Krämer, M.; Krutzsch, B.; Pischinger, S.; Voigtländer, D.; Wenninger, G.; Wirbeleit, F.; Brogan, M.S.; Brisley, R.J.; Webster, D.E. Removal of nitrogen oxides from the exhaust of a lean-tune gasoline engine. *Appl. Catal.* **1995**, *7*, 153–171. [CrossRef]
8. Wang, J.; Wu, C.; Chen, J.; Zhang, H. Denitrification removal of nitric oxide in a rotating drum biofilter. *Chem. Eng. J.* **2006**, *121*, 45–49. [CrossRef]
9. Chen, J.M.; Ma, J.F. Abiotic and biological mechanisms of nitric oxide removal from waste air in biotrickling filters. *J. Air Waste Manag. Assoc.* **2006**, *56*, 32–36. [CrossRef]
10. Ramirez, M.; Gómez, J.M.; Aroca, G.; Cantero, D. Removal of hydrogen sulfide by immobilized Thiobacillus thioparus in a biotrickling filter packed with polyurethane foam. *Bioresour. Technol.* **2009**, *100*, 4989–4995. [CrossRef]
11. Philip, L.; Deshusses, M.A. Sulfur dioxide treatment from flue gases using a biotrickling filter-bioreactor system. *Environ. Sci. Technol.* **2003**, *37*, 1978–1982. [CrossRef]
12. Jiang, R.; Huang, S.; Chow, A.T.; Yang, J. Nitric oxide removal from flue gas with a biotrickling filter using Pseudomonas putida. *J. Hazard. Mater.* **2009**, *164*, 432–441. [CrossRef]
13. Liang, W.; Huang, S.; Yang, Y.; Jiang, R. Experimental and modeling study on nitric oxide removal in a biotrickling filter using Chelatococcus daeguensis under thermophilic condition. *Bioresour. Technol.* **2012**, *125*, 82–87. [CrossRef] [PubMed]
14. Flanagan, W.P.; Apel, W.A.; Barnes, J.M.; Lee, B.D. Development of gas phase bioreactors for the removal of nitrogen oxides from synthetic flue gas streams. *Fuel* **2002**, *81*, 1953–1961. [CrossRef]
15. Lee, B.D.; Apel, W.A.; Smith, W.A. Oxygen effects on thermophilic microbial populations in biofilter treating nitric oxide containing off-gasstreams. *Environ. Prog.* **2001**, *20*, 157–166. [CrossRef]
16. Caceres, M.; Silva, J.; Morales, M.; San, R.M.; Aroca, G. Kinetics of the biooxidation of volatile reduced sulphur compounds in a biotrickling filter. *Bioresour. Technol.* **2012**, *118*, 243–248. [CrossRef]
17. Song, J.; Kinney, K.A. A model to predict long-term performance of vapor phase bioreactors: A cellular automation approach. *Environ. Sci. Technol.* **2002**, *36*, 2498–2507. [CrossRef]
18. Zarook, S.M.; Shaikh, A.A. Analysis and comparison of biofilter modes. *Chem. Eng. J.* **1997**, *65*, 55–61. [CrossRef]
19. Meena, V.; Rajendran, L. Analytical expression of concentration profiles of methanol and pinene in air stream and bio-film phase. *J. Anal. Bioanal. Tech.* **2014**, *6*, 1–8.
20. Meena, V.; Rajendran, L.; Kumar, S.; Jansi Rani, P.G. Mathematical modeling of gas phase and biofilm phase biofilter performance. *Egypt J. Basic Appl. Sci.* **2016**, *3*, 94–105. [CrossRef]
21. Deshusses, M.A.; Hamer, G.; Dunn, I.J. Behavior of biofilters for waste air biotreatment. 1. Dynamic model development. *Environ. Sci. Technol.* **1995**, *29*, 1048–1058. [CrossRef]
22. Liao, Q.; Chen, R.; Zhu, X. Theoretical model for removal of volatile organic compound (VOC) air pollutant in trickling biofilter. *Sci. China Ser. E* **2003**, *46*, 245–258. [CrossRef]
23. Manimegalai, B.; Lyons, M.E.G.; Rajendran, L. A kinetic model for amperometric immobilized enzymes at planar, cylindrical and spherical electrodes: The Akbari-Ganji method. *J. Electroanal. Chem.* **2021**, *880*, 114921. [CrossRef]
24. Selvi, M.S.M.; Rajendran, L.; Abukhaled, M. Estimation of rolling motion of ship in random beam seas by efficient analytical and numerical approaches. *J. Mar. Sci. Appl.* **2021**, *20*, 55–66. [CrossRef]
25. Chitra Devi, M.; Pirabaharan, P.; Rajendran, L.; Abukhaled, M. Amperometric biosensors in an uncompetitive inhibition process: A complete theoretical and numerical analysis. *React. Kinet. Mech. Catal.* **2021**, *133*, 655–668. [CrossRef]
26. Saranya, K.; Mohan, V.; Rajendran, L. Steady state concentrations of carbon dioxide absorbed into phenyl glycidyl ether solutions by residual method. *J. Math. Chem.* **2020**, *58*, 1230–1246. [CrossRef]
27. Joy Salomi, R.; Vinolyn Sylvia, S.; Rajendran, L.; Abukhaled, M. Electric potential and surface oxygen ion density for planar, spherical and cylindrical metal oxide grains. *Sens. Actuators B Chem.* **2020**, *321*, 128576. [CrossRef]
28. Joy Salomi, R.; Vinolyn Sylvia, S.; Rajendran, L.; Lyons, M.E.G. Transient current, sensitivity and resistance of biosensors acting in a trigger mode: Theoretical study. *J. Electroanal. Chem.* **2021**, *895*, 115421. [CrossRef]
29. Manimegalai, B.; Rajendran, L.; Lyons, M.E.G. Theory of the Transient Current Response for the Homogeneous Mediated Enzyme Catalytic Mechanism at the Rotating Disc Electrode. *Int. J. Electrochem. Sci.* **2021**, *16*, 210946. [CrossRef]
30. Lyons, M.E.G. Understanding the kinetics of catalysed reactions in microheterogeneous thin film electrodes. *J. Electroanal. Chem.* **2020**, *872*, 114278. [CrossRef]
31. Chitra Devi, M.; Pirabaharan, P.; Lyons, M.E.G.; Rajendran, L. Investigation of the Diffusion Impedance for an Irreversible Redox Reaction. *Int. J. Electrochem. Sci.* **2021**, *16*, 210639. [CrossRef]
32. Akbari, M.R.; Ganji, D.D.; Nimafar, M.; Ahmadi, R. Significant progress in solution of nonlinear equations at displacement of structure and heat transfer extended surface by new AGM approach. *Front. Mech. Eng.* **2014**, *9*, 390–401. [CrossRef]
33. Jeyabarathi, P.; Rajendran, L.; Lyons, M.E.G. Reaction-diffusion in a packed-bed reactors: Enzymatic isomerization with Michaelis-Menten Kinetics. *J. Electroanal. Chem.* **2022**, *910*, 116184. [CrossRef]
34. Akbari, M.R.; Nimafar, M.; Ganji, D.D.; Karimi Chalmiani, H. Investigation on non-linear vibration in arched beam for bridges construction via AGM method. *Appl. Math. Comput.* **2017**, *298*, 95–110. [CrossRef]
35. Meresht, N.B.; Ganji, D.D. Solving nonlinear differential equation arising in dynamical systems by AGM. *Int. J. Appl. Comput. Math.* **2017**, *3*, 1507–1523. [CrossRef]
36. Rasi, M.; Kumar, S.; Rajendran, L. Analytical expressions for the concentration of nitric oxide removal in the gas and biofilm phase in a biotrickling filter. *J. Assoc. Arab Univ. Basic Appl. Sci.* **2015**, *18*, 19–28.

37. Jeyabarathi, P.; Kannan, M.; Rajendran, L. Mathematical Model for Extracting Hollow Fiber Membrane Contactors from Carbon dioxide using Adomian decomposition method. *Int. J. Sci. Res.* **2020**, *9*, 6230–6233.
38. He, J.H.; El-Dib, Y. Homotopy perturbation method for Fangzhu oscillator. *J. Math. Chem.* **2020**, *58*, 2245–2253. [CrossRef]
39. He, J.H.; El-Dib, Y. Homotopy perturbation method with three expansions. *J. Math. Chem.* **2021**, *59*, 1139–1150. [CrossRef]
40. Ali, M.; Anjum, N.; Ain, Q.T.; He, J.H. Homotopy perturbation method for the attachment oscillator arising in nanotechnology. *Fibers Polym.* **2021**, *22*, 1601–1606. [CrossRef]
41. He, J.H.; El-Dib, Y.O.; Mady, A.A. Homotopy Perturbation Method for the Fractal Toda Oscillator. *Fractal Fract.* **2021**, *5*, 93. [CrossRef]
42. He, J.H.; Ji, F.Y. Taylor series solution for Lane–Emden equation. *J. Math. Chem.* **2019**, *57*, 1932–1934. [CrossRef]
43. Jeyabarathi, P.; Rajendran, L.; Abukhaled, M.; Kannan, M. Semi-analytical expressions for the concentrations and effectiveness factor for the three general catalysts shapes. *React. Kinet. Mech. Catal.* **2022**, 1–16. [CrossRef]
44. Vinolyn Sylvia, S.; Joy Salomi, R.; Rajendran, L.; Abukhaled, M. Solving nonlinear reaction–diffusion problem in electrostatic interaction with reaction-generated pH change on the kinetics of immobilized enzyme systems using Taylor series method. *J. Math. Chem.* **2019**, *59*, 1332–1347. [CrossRef]
45. Wazwaz, A.M. Optical bright and dark soliton solutions for coupled nonlinear Schrödinger (CNLS) equations by the variational iteration method. *Optik* **2020**, *207*, 164457. [CrossRef]
46. Nirmala, K.; Manimegalai, B.; Rajendran, L. Steady-State Substrate and Product Concentrations for Non Michaelis-Menten Kinetics in an Amperometric Biosensor—Hyperbolic Function and Padé Approximants Method. *Int. J. Electrochem. Sci.* **2020**, *15*, 5682–5697. [CrossRef]
47. Namihira, T.; Tsukamoto, S.; Wang, D.; Katsuki, S.; Hackam, R.; Akiyama, H.; Uchida, Y.; Koike, M. Imrovement of NO_X removal efficiency using short-width pulsed power. *IEEE Trans. Plasm. Sci.* **2000**, *28*, 434–442. [CrossRef]
48. Deshusses, M.A.; Webster, T.S. Construction and economics of a pilot/full-scale biological trickling filter reactor for the removal of volatile organic compounds from polluted air. *J. Air Waste Manag. Assoc.* **2000**, *50*, 1947–1956. [CrossRef]
49. Hodge, D.S.; Devinny, J.S. Modeling removal of air contaminants by biofiltration. *J. Environ. Eng. Sci.* **1995**, *121*, 21–32. [CrossRef]
50. Iranpour, R.; Cox, H.H.J.; Deshusses, M.A.; Schroeder, E.D. Literature review of air pollution control biofilters and biotrickling filters for odor and volatile organic compound removal. *Environ. Prog.* **2005**, *24*, 254–267. [CrossRef]
51. Khan, F.I.; Ghoshal, A.K. Removal of volatile organic compounds from polluted ai. *J. Loss Prev. Process. Ind.* **2000**, *13*, 527–545. [CrossRef]
52. Han, Y.; Zhang, W.; Xu, J. A simplified mathematical model of multi-species biofilm for simultaneous removal of sulfur dioxide (SO_2) and nitric oxide (NO) using a biotrickling-filter. *Afr. J. Microbiol. Res.* **2011**, *5*, 541–550.